Summer 6-10-2022

Studies in the use of 1,1'-di(1-hydroxyethyl)ferrocene as a Flame Retardant for Polyurethanes

Chanel Yeary
Pittsburg State University, c.yeary21@gmail.com

STUDIES IN THE USE OF 1,1'-DI(1-HYDROXYETHYL) FERROCENE AS A FLAME RETARDANT FOR POLYURETHANES

A Thesis Submitted to the Graduate
School in Partial Fulfillment of the
Requirements for the Degree of
Master of Science

Tabytha Chanel Yeary

Pittsburg State University

Pittsburg, Kansas

July, 2023

STUDIES IN THE USE OF 1,1'-*BIS*(1-HYDROXYETHYL) FERROCENE AS A FLAME RETARDANT FOR POLYURETHANES

Tabytha Chanel Yeary

APPROVED:

Thesis Advisor _____
Dr. Charles Neef, Chemistry Department

Committee Member _____
Dr. Ram Gupta, Chemistry Department

Committee Member _____
Dr. Irene Zegar, Chemistry Department

Committee Member _____
Dr. Jeanne Norton, Engineering Technology Department

ACKNOWLEDGEMENTS

I'd like to start by thanking my friends and family who have supported and loved me through this entire journey. These amazing people allowed me to realize my dream through their support and encouragement. I'd also like to give a special thank you to Dr. Jody Neef. Through his guidance and mentorship, I have gained the skills that have allowed me to become the chemist I am proud to be today.

In addition, I would like to acknowledge the Pittstate Chemistry Department for their financial support and facilities have allowed me to achieve my degree. Thank you to all the professors and faculty have supported me through this process and allowed me the opportunity to gain the skills I've needed over the years. Further thanks to Dr. Ram Gupta, Dr. Irene Zegar, Dr. Jeanne Norton, and Dr. Khamis Siam for sitting on my thesis committee. Their willingness to take time out of their schedule to read and review my thesis is greatly appreciated.

Finally, I'd like to thank all the amazing women before me who paved the way and allowed me to see that a woman like me can do anything she puts her mind to.

STUDIES IN THE USE OF 1,1'-*BIS*(1-HYDROXYETHYL)FERROCENE AS A FLAME RETARDANT FOR POLYURETHANES

An Abstract of Thesis by
Tabytha Chanel Yeary

Significant research in non-toxic flame retardants (FRs) has been performed in recent years since the dangerous consequences of halogenated FR were found. As early as the 1970's, carcinogenic the side effects of halogenated compounds were being acknowledged. Since the early 2000's halogenated FRs began being phased out of use due to these negative side effects. Since then, significant research continued in exploring alternative effective flame retardants. Ferrocene (Fc) has shown to be a promising alternative to halogenated FRs due to its nontoxicity and FR properties. This research reports on the synthesis of 1,1'-di(1-hydoxyethyl) ferrocene (DHEFc) and its incorporation into a polyurethane. A study of the flame retardant properties of DHEFc and/or Halloysite were explored using varying amounts of DHEFc and/or Halloysite that were then combined with BiOH 2100 followed by toluene di-isocyanate. The mixtures were poured onto a glass pane and drawn with a doctor's blade to form thin films. FT-IR spectra, H-NMR, COSY, thermal stability by TGA, and horizontal flame testing of the films were reported.

TABLE OF CONTENTS

LIST OF TABLES

TABLE PAGE

LIST OF FIGURES

FIGURE PAGE

LIST OF SCHEMES

SCHEME PAGE

CHAPTER I

INTRODUCTION

1.1 Polyurethanes (PU)

In 1849 Dr. Wrurtz was the first individual to report a synthesis route for urethanes. His work was further enhanced in 1937, by Otto Bayer who was the first individual to use a polyester diol and a diisocyanate to synthesize PUs in Germany[1,2]. This major contribution to the field added a new class to polymerization called polyaddition. While this discovery was a breakthrough of the time, Bayer's PU was largely limited in its application. Modern day PU's are formed by hydroxyl groups (OH) and (NCO) groups of isocyanates.

This novel synthesis was used to develop a global multibillion dollar industry. As of 2020 worldwide PU grossed 56.45 billion dollars and projected to increase 5.1% from 2020 -2028[3], PU's are used within the market in various forms such as elastomers, molded foam,

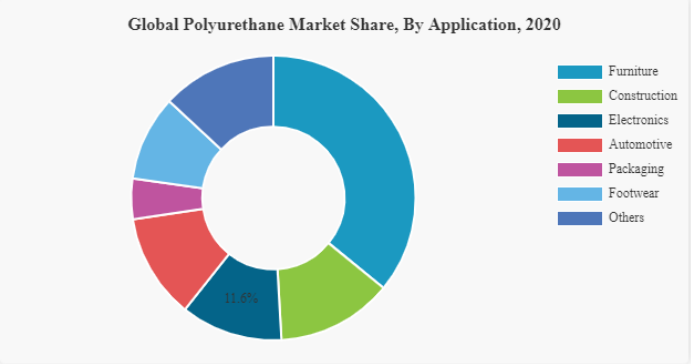

Figure 1: Global Polyurethane Applications 2020[3]

coatings, and others based on the form needed. A 2020 report of global PU market shares by application and determined furniture was the largest applications of PU (Figure 1) driving the need for flexible polyurethane foams (PUF). Characteristics of PUF's such as being lightweight, durable, and resilient, as well as non-allergenic and flexible makes obvious why it dominates the furniture industry. In contrast to the benefits PUF's have contributed to society an average of 3,170 deaths in America per year are attributed to fires[4]. It was found in 2018 that of those 3,170 deaths , 16.30% were residential fires where PUF's are prolifically used in furniture, bedding etc. Considering these disturbing statistics, research has focused on flame retardants to curtail fire related deaths.

To understand the characteristics of an effective flame retardant, the decomposition of PUs is vital to the process. When PUs are exposed to a heat source, pyrolysis of the polymer results in flammable gases being released. These gases result in highly toxic smoke, especially carbon monoxide and hydrogen cyanide. Beyond the environmental and acute health concerns, these gases, when combined with the oxygen in the atmosphere, an adequate environment for the ignition of the polymer is created. Once combustion is achieved a feedback system occurs, producing heat that spreads and fed back into the system (Figure 2)[5]. This continues the pyrolysis of the polymer by furthering the combustion cycle. To help

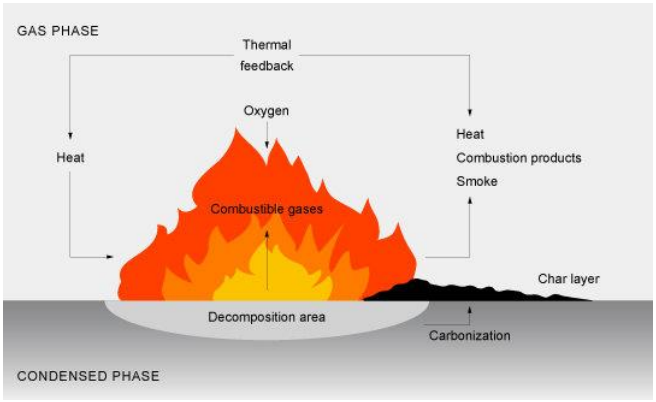

Figure 2: Pyrolysis Combustion Cycle[4]

resolve the pyrolysis feedback loop in PU, there continues to be significant research into flame retardants that are capable of inhibiting or suppressing the combustion process.

1.2 Evolution of Flame Retardants (FRs)

Flame retardants have four major types of mechanisms[6]: (1) The vapor phase of a fire proceed via oxide/hydroxide radicals produced by the fire. These radicals can form toxic gasses. As a metal, ferrocene is capable of forming metal oxide/salt compounds possessing the capability to go through various states of oxidation generating radicals that can suppress the oxide/hydroxide radicals produced by the fire. (2) Dilution is another mechanism in which hydrated minerals can exploit the endothermic reaction that is occurring once the system is heated. (3) Char is the two-fold process that quenches the physical polymer by transforming into cross linked structures. These compounds are nitrogen based with a two-fold advantage of suppressing the toxic vapor as well as act as a protective shield from the PU below. (4) Lastly, intumescence the process where spumific compounds decompose to larger quantities of a non-combustible gas which possess carbon and acid donors that result in a foam that solidifies though cross-link reactions[7].

FRs are formulated into a polymer as either additives or reactant compounds. Using simple additives as FRs by incorporating them into a coating is beneficial financially, but disadvantages such as poor compatibility, loss of mechanical strength and leaching can be problematic in their efficacy. Reactive FRs, such as functionalized ferrocene, can utilize flame retardant functional groups copolymerized within the polymer to create a matrix where polymers cannot easily migrate out of the weakly bound additive FR. There

are two major forms of reactive FRs, (1) Halogenated FRs and (2) Non-halogenated FR.

1.2.1 Halogenated Flame Retardants

In the 1970's halogenated FRs were found to have effective flame-retardant properties. Brominated flame retardants (BFRs) were a found to have desirable characteristics for flame retardancy and was found that lower energy bromine radicals can replace the active chain carriers, slowing the rate of energy and therefore extinguishing the flame within the vapor phase (Figure 3)[8], however, these positive results came with a large cost.

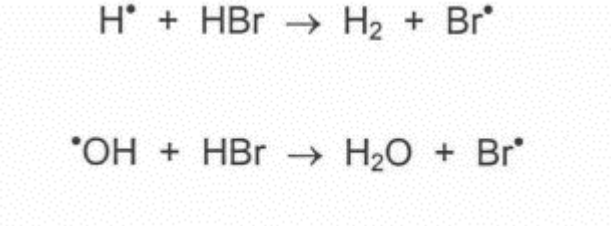

Figure 3: Halogenated Flame Retardant Mechanism[8]

Polybrominated diphenyl ethers (PBDEs) are a widely known and were one of the most popular FRs in furniture foams and electronics[9,10]. In 2008, Environmental Working Group (EWG) concluded a five-year study of breast milk, maternal blood, and umbilical cord samples. Five different types of PBDEs were present with three of the five PBDEs being more prone to being present in the infant in comparison to the mother[10]. Dr. Amina Salamova, lead author of the study, commented she expected to "see lower levels with these chemicals being banned for a decade" [11]. This research has fueled further studies that have linked PBDEs to serious learning, mental and developmental problems in children as well as affecting the endocrine system and cancer in both animal and epidemiological studies.

1.2.2 Non-halogenated Flame Retardants

Non-halogenated flame retardants became a significant area of research in response to halogenated flame retardants. Recent developments have generated various methods of flame suppression.

1.2.3 Phosphorus Based Flame Retardants (P-FRs)

Once halogenated flame retardants were banned, intense research was put into effective non-halogenated flame-retardant replacements. Research into phosphorous based FRs were considered due to phosphorous possessing chemical versatility allowing for multiple FR mechanisms. P-FRs showed efficacy in impacting the condensed phase through dehydrating the polymeric structure which in turn would form a char layer to suppress the release of volatiles while other P-FRs were able to act through intumesces that slowed down the heat transfer to the material.

Furthermore, inorganic FRs such as $Al(OH)_3$, have been shown to be capable of effecting pyrolysis in two different fashions by impacting the gas-phase when acting in parallel to the condensed-phase mechanism. P-FRs has been shown to have a similar ability to impact the release of hydrogen and hydroxide radicals that propagate during the combustion cycle. P-FRs can produce phosphorous radicals that attract hydroxide radicals lowering their concentration in a process known as flame poisoning. This led to organophosphorus flame retardants (OPFRs) being currently studied as a substitute for brominated FRs[11,12].

OPFRs are of particular interest since they are used as an additive rather than chemically bonded to the polymer matrix. This field of work was initially investigated by Kirman, J. in 1964 through his understanding of the radical mechanism[12]. His work

was built upon by Beach et al. through demonstrating the radical process suggesting a mechanism for FRs containing bromine and sulfur as an additive for polystyrene[13]. This team reported sulfur based FRs with triphenyl phosphate yielded results comparable to hexabromocyclododecane (HBCD). As of 2013, Wagner et al. reported on the synergistic efficacy of OPRFs and synergists containing disulfide bridges when in polystyrene matrices[14]. This provided further confirmation of OPFRs went through a radical decomposition mechanism within the polymer.

Most recently P-FRs with heteroatoms, particularly P-N interactions, have been the most promising in flame retardancy synergism with no presence of halogenation. The P-N bond is known to be a cross-link promoter which in turn encourages the polymer to retain the phosphorous in the condensed phase encouraging a char layer to form with higher yield as well as that char being more thermally stable. Currently phosphonamidites and cyclotryphosphazenes are exhibiting this characteristic with promising results[13].

1.2.4 Metal Oxide Based Flame Retardants

Metal oxides were reported to work well with other flame retardants, specifically TiO_2 and Al_2O_3 in poly(methyl methacrylate)(PMMA) as well as Al_2O_3 and Fe_2O_3 combined with a red phosphorous in recycled poly(ethylene terephthalate)(PET). It was found that considering Al_2O_3 not being a transition metal provided some key information for the work to come. It was determined that PMMA when combined with either of the nanoscale components and an aluminum organophosphate the Al_2O_3 was generally more successful at flame retardancy than TiO_2. It was noted that the Al_2O_3 performed better, with its primary mechanism of flame retardancy being grounded in a charring.

mechanism that exhibited less cracks and openings than compared to the TiO_2. It was seen that TiO_2 was only more effective when coming to smoke suppression[15].

As of 2009, Morgan reviewed a metal salt flame retardancy system using a wide range of iron phosphates, oxides, borates, and silicates while in combination with a charring polymer (polyphenylene oxide, PPO) and zinc borate[15]. When the iron compounds were singularly used, flame retardancy was not improved much at all but became more effective when in combination with either of the charring agents. It was determined via X-ray diffraction that redox chemistry had occurred during the combustion process leading to improved flame retardancy. The authors did point out that the conditions seen during combustion led to *in-situ* formation of $Fe(CO)_5$ that is known to be a successful vapor phase FR. A series of experiments studying the flame inhibition of transition metals, specifically, Fe, Sn, and Mn was reported on for their viability as FRs. It was founded that the $Fe(CO)_5$ was the most effective metal-based flame inhibitor followed by Mn and Sn when compared to brominated FR[15]. The various oxidation states of the intermediaries formed during combustion influenced the vapor phase chemistry before they reached their final oxide or hydroxide states. It was noted that these results were only in the vapor phase and not the burning polymer itself. These exciting results were quickly shown to be just as toxic as their predecessors but did provide examples of transition metals as flame retardants. The study noted that Fc showed similar flame inhibition without the toxicity of $Fe(CO)_5$ or other organometallics[15].

1.3 Modern Non-Halogenated FRs

1.3.1 Graphene Sheet Flame Retardants

One of the more recent and effective FR discoveries has been in the nanomaterial material science field. When graphene is incorporated into a polymer matrix the resulting nanocomposites were observed to possess flame retardancy properties[19]. Wang Q et al. prepared a synthetic route for graphene sheets decorated with 10-oxide-g-(2,3-epoxypropoxy) propyltrimethoxysilane (DPP)[19]. These compounds were incorporated into epoxy samples (EP). Results were discussed comparing the flame retardancy of non-FR EP, DPP/EP and DPP-GO/EP. Figure 3 details the morphologies of the epoxy (EP) samples and SEM images of outer and inner layers of the carbonized DPP-GO/EP. The imaging confirmed the successful carbonization of the sample and was thus burn tested. The group proposed the system went through a char mechanism. The flame retardancy mechanism proposed unravels in a two-fold fashion. The graphene sheets initially form an inner layer physical protective char while in the late stages of combustion the DPP decoration chemically forms a char encapsulating the GO and creates a protective barrier. This development in flame retardant research has been found to be effective and sustainable though cost is still a concern to be considered.

1.4 Ferrocene and Flame Retardancy Properties

Ferrocene (Fc) is a name coined by Woodward and Whitting , who disclosed the sandwich structure in 1952[20]. Further research revealed that ferrocene had notable characteristics, displaying high thermal stability, mild and reversible oxidation as well as reactivity. Initial studies of ferrocene were a continuation of work exploring the flame-retardant properties of $Fe(CO)_5$. As stated earlier, iron pentacarbonyl was found to be highly effective as a FR when compared to halogenated but was still found to be highly toxic when a part of the combustion cycle.

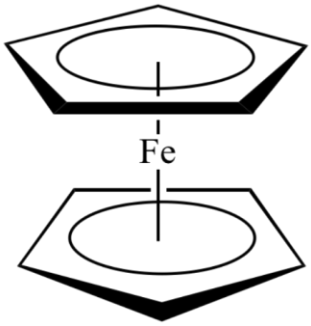

Figure 4: Ferrocene Molecule Structure

Ferrocene was proposed as the non-toxic solution to introducing iron atoms into the system. It was determined iron pentacarbonyl and ferrocene undergo the same sub-mechanisms thus the flame reduction speed is similar[20]. In the gas phase of combustion, ferrocene molecules release iron atoms. These in turn react O_2 to form FeO_2 which is further reduced to FeO, a long lived intermediate[20]. This intermediate along with $Fe(OH)_2$ enters a catalytic cycle providing H-atom recombination and allows Fe to remove radicals that propagate the combustion cycle in the gas phase. Linteris et al. reported this work concluding that Fc was used in place of $Fe(CO)_5$, Fc was shown that in smaller mole fractions it was an effective flame retardant in the gas phase however it was noted that the FR efficacy diminished with increasing mole fractions. It was proposed that Fc in combination with other thermal inhibiters would help mitigate the necessity of a large Fc mole fraction[20].

$$\mathrm{FeOH + H \leftrightarrow FeO + H_2}$$
$$\mathrm{FeO + H_2O \leftrightarrow Fe(OH)_2}$$
$$\mathrm{Fe(OH)_2 + H \leftrightarrow FeOH + H_2O}$$
$$\mathrm{(net:\ H + H \leftrightarrow H_2)}$$

Scheme 1: Iron Sub-mechanism[20]

1.5 Halloysite Nanotubes Flame Retardancy Properties

Halloysite nanotubes (HNT) were first reported by Berthier in 1826 as a 1:1 clay mineral from the kaolin group[21]. HNT is found world-wide and comes in a variety of morphologies, though tubular halloysite is the most common as well as the most sought after for applications. These nanotubes can be classified into two groups: (1) hydrated with a crystalline structure possessing 10 Å spacing and (2) dehydrated crystalline structure possessing a crystalline structure of 7 Å spacing. This irreversible physical change through dehydration is one of the most important distinctions between HNTs and kaolin. This physical change allows for many of the hydroxyl groups present to be concentrated on the internal side of the HNT thus creating an outside layer of Si-O-Si bonds (Figure 5)[23]. This lack of hydroxyl groups allows for HNTs to easily disperse in the PU that ultimately promotes flame retardancy behavior. However, Vahabi and his team reported that there were difficulties in dispersion with high levels of HNTs which necessitated the need of functionalization to achieve optimal thermal stability. HNTs impact the combustion cycle through creating a char layer that will suppress the fuel source of the flame, however it is known that raw HNTs are inefficient in their ability to retain the thermal stability. This in turn has sparked a discussion on HNT and synergism with other flame retardants. The obvious place to start research was with the phosphorous flame

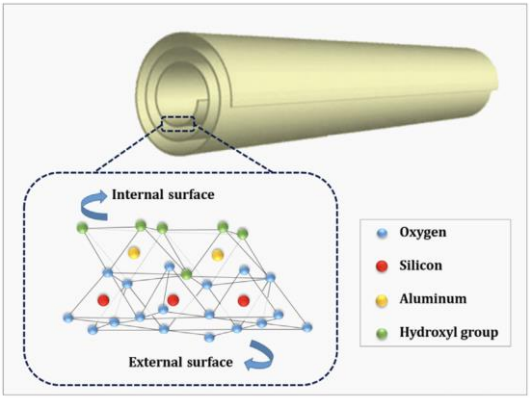

Figure 5: Halloysite Nanotube Diagram[22]

retardants that are forming aluminosilicate phosphates derived from the aluminosilicate backbone of the HNTs. It was reported that thermal and structural improvements enhancing the barrier effect of the char layer. Further research in synergistic effects of flame retardants and HNTs is an area of research to be expanded upon[22,23].

1.6 Project Rationale

Halogenated flame retardants are being phased out of use due to their toxicity and bio-persistence which necessitates the need for effective, bio-friendly, and non-halogenated alternatives. This study proposes the use of a ferrocene diol as an alternative to halogenated flame retardants for use in polyurethanes. When introduced into a polyurethane, the ferrocene is expected to generate lower energy iron radicals that suppress the vapor phase of the pyrolysis cycle. In addition, ferrocene has been shown to be an effective charring agent. In conjunction, the combination of the ferrocene diol and halloysite will be studied to compare the char efficacy of the two additives. Furthermore, the flame-retardant efficacy of ferrocene and halloysite when used in tandem was explored for possible synergistic effects.

The ferrocene diol will be synthesized in two steps by deacetylation of ferrocene followed by reduction with sodium borohydride to produce 1,1-di(1-hydroxyethyl)ferrocene (DHEFc). Polyurethane films will then be prepared with various amounts of DHEFc and commercially available polyols and isocyanates. Each film will be tested using a vertical flame test (VFT) and thermal gravimetric analysis (TGA).

CHAPTER II

EXPERIMENTAL

2.1 Materials & Methods

All materials used are as follows: ferrocene (Alter Aesar), halloysite (Aldrich), sodium borohydride (TCI Chemicals), dichloromethane (Acros Organic), tetrahydrofuran (Acros Organic), and isopropyl alcohol (Acros Organic). Polyol and isocyanate were obtained from ETCO-Specialty Products Inc. in Girard.

2.2 Horizontal Flame Testing

All horizontal flame testing was performed adhering to ASTM D-635 standards using a M233M Vertical Flame Chamber[18] Representative samples (1 in x 5 in x 3mm) were generated and placed in horizontal chamber. A flame was applied for 10 seconds and then allowed to burn until flame was no longer observed. Burn time, mass post burning, and any char residue was recorded.

2.3 Thermogravimetric Analysis

A TA Instruments thermogravimetric spectrometer was used to obtain characterization of thin films. Each sample was analyzed from room temperature to 600^{o}C with 10^{o}C/min ramp rate.

Further characterization was performed using Perkin Elmer Spectrum Two Fourier Transform Infrared Spectrometer and Bruker DPX-300 NMR Spectrometer.

2.4 Synthesis of 1,1-*di*(hydroxyethyl)ferrocene & Formulations

2.4.1 Synthesis of 1,1-diacetylferrocene (DAF) [24]

Dichloromethane (300 mL) was placed in an Erlenmeyer flask along with aluminum chloride (18.8 g, 0.141 mol) and acetyl chloride (12.1 g, 0.154 mol). The solution was allowed to stir for 30 minutes. Over a period of 20 minutes, ferrocene (10.0 g, 0.054 mol) was slowly added to the solution and then allowed to react for 16 hours. The solution was neutralized via pouring the solution over ice and organic phase was separated and obtained. The crude product was recrystallized in 100 mL of isopropyl alcohol. The crystals were collected using vacuum filtration and dried in vacuum oven overnight. Yield: 19.1g (95.5%). ^{1}H-NMR (ppm): 4.781, 4.530, 2.368, 1.251. FT-IR (cm^{-1}): 2971, 1726.

2.4.2 Synthesis of 1,1'-di(1-hydroxyethyl)ferrocene (DHEFc)[24]

The reduction of DAF was accomplished by modification of a literature procedure[19]. Reaction time, sodium borohydride and solvent were studied to optimize the reaction system. The procedure which resulted in the highest yield is detailed below:

DAF (5.00 g, 0.0185) along with sodium borohydride (2.12 g, 0.055 mol) was placed in a conical flask. A 1:3 ratio of tetrahydrofuran (125 mL) and isopropyl alcohol (375 mL) were added to the flask. The red solution was allowed to react for 16 hours. Once the reaction was complete, the solution was extracted via brine (250 mL) and diethyl ether (125 mL), stirring another 30 minutes. The organic phase was collected using a separatory funnel and dried over sodium sulfate. The solution was filtered

through alumina silicate column and solvent was removed via rotary evaporator. The yellow product was placed under reduced pressure overnight. Yield: 1.88g (62.6%) ^{1}H-NMR (ppm): 7.240, 4.138, 1.444 FT-IR (cm^{-1}): 3289.2, 1651.3.

2.4.3 Synthesis of Polyurethane Thin Films

A typical procedure for polyurethane films **(**amounts of DHEFc and/or halloysite varying from 0-30%) is as follows: polyol (11.25 g, 0.02076 mol) and DHEFc and/or Halloysite (1.25 g, 0.00463 mol) were thoroughly blended (Table 1). Once combined, di-isocyanate (3.85g, 0.0285 mol) was added, and the mixture stirred for 40-60 sec. The samples were then cast into thin films onto a glass plate, using a doctor's blade[26] (Figure 6). The films were allowed to cure for two hours at room temperature and then placed into an oven at 60 ^{o}C for 12 hours. FT-IR (cm^{-1}): 3000, 2970, 2870 and 1726.

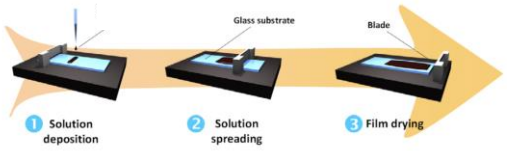

Figure 6: Thin-Film Casting Diagram[25]

CHAPTER III

RESULTS AND DISCUSSION

3.1 Synthesis of 1,1-di(hydroxyethyl)ferrocene (DHEFc)

DHEFc was synthesized in two steps beginning with ferrocene (Scheme 2). An acetylation of ferrocene gave a high yield of 1,1'-DAF. However, the reduction of the ketone to an alcohol was more difficulty than indicated in literature and further studies were performed to optimize this reaction.

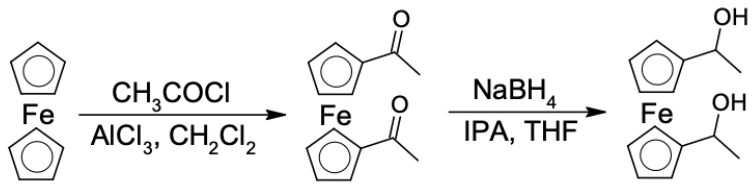

Scheme 2: Synthesis of DHEFc

3.1.1 Synthesis of 1,1'-DAF

1,1'-DAF was synthesized by reacting ferrocene with acetyl chloride under Friedel-Crafts conditions. After recrystallization from IPA, 1,1'-DAF was obtained in an excellent yield of 95.5%. An FT-IR spectrum of the product confirmed the presence of C-H stretching seen at 2971 cm^{-1} and a carbonyl peak occurring at 1663 cm^{-1} (Figure 7). The

weak stretch observed at 3400 cm^{-1} was attributed to trace amounts of isopropyl alcohol post recrystallization.

A proton NMR spectrum (Figure 8) of 1,1'-DAF was obtained and confirmed the presence of ferrocenyl protons at 4.781 ppm and 4.530 ppm. The chemical shifts of the ferrocenyl protons are further upfield than typical aromatic protons due to the cyclopentadiene rings possessing a negative charge which shields these protons. The methyl protons appeared at 2.368 ppm which was consistent with their proximity to the carbonyl. The integration was 2:2:3 which was consistent with the structure of 1,1'-DAF.

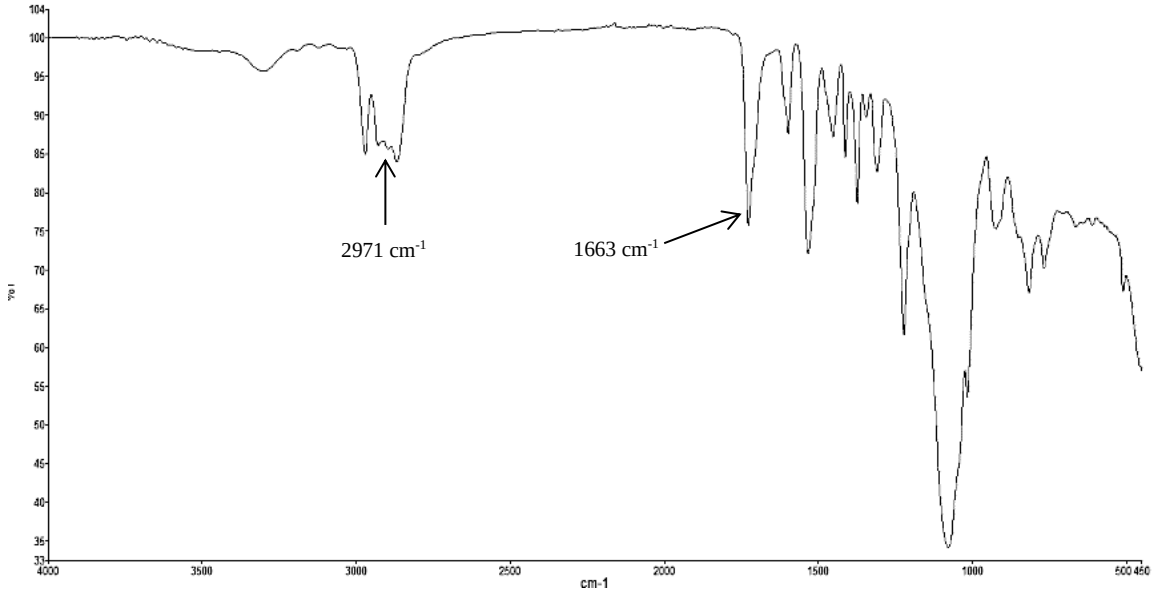

Figure 7: FT-IR Spectrum of 1,1'-DAF

3.1.2 Optimization of DHEFc Synthesis

The initial synthesis of DHEFc was according to a literature method with $NaBH_4$ using IPA as the solvent. However, after completion of the reaction a significant carbonyl stretch was observed in the IR spectrum, indicating a full reduction had not occurred (Figure 9). The lack of reduction was attributed to the limited solubility of ferrocene in IPA. In addition, the reactivity of the carbonyl is less compared to other carbonyls due to the electron richness of ferrocene. The strong electron donation of ferrocene decreases the partial positive charge on the carbonyl carbon, resulting in a low electrophilicity. To optimize the yield of the DHEFc two reaction conditions were studied: solvent and $NaBH_4$ amount.

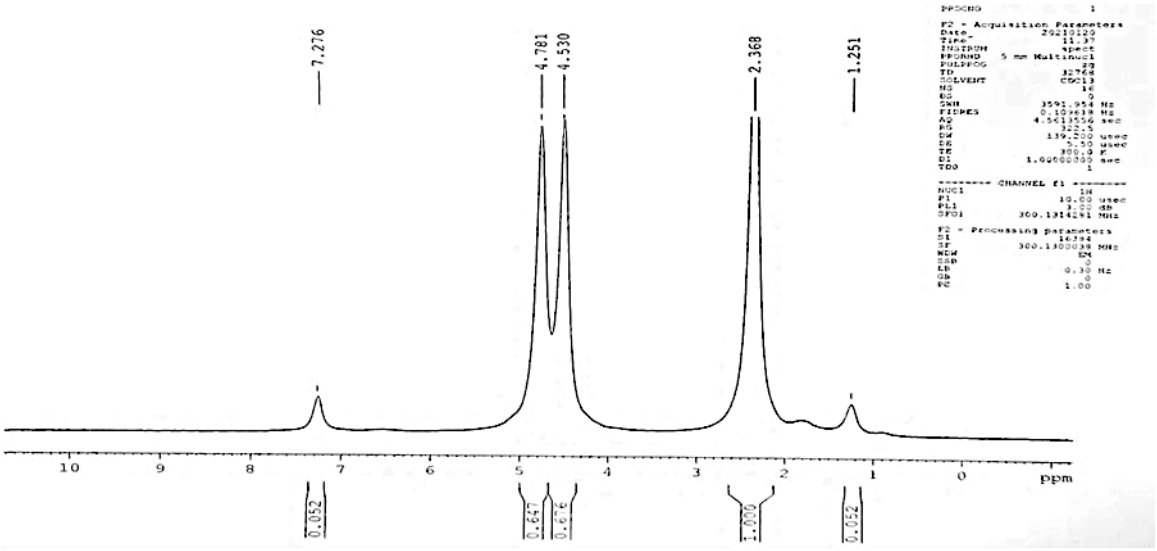

Figure 8: ^{1}H-NMR Spectrum of 1,1'-DAF

3.1.3 Solvent Effects

To increase the solubility of 1,1'-DAF during reduction, THF was chosen as a co-solvent. THF is a good solvent for 1,1'-DAF and has been used previously for carbonyl reduction reactions[47]. For this study, the amount of THF was varied from 0 to 75% and the ratio of 1.1'-DAF to $NaBH_4$ was held constant at 1:2 molar ratio. Reaction times were 24h (Table 1).

Table 1: Solvent Study Parameters

Trial	% THF	O-H (%T*)	C=O (%T*)
1	0	83	72
2	25	78	86
3	50	86	84
4	75	97	87

* % transmittance

Following completion of each reaction, an IR spectrum of the crude product was obtained and the % transmittance of the O-H stretch at 3320 cm^{-1} and the C=O stretch at 1663 cm^{-1} were compared. In Trial 1 (0% THF), the % transmittance of the O-H stretch and the C=O stretch were 83 and 72%, respectively (Figure 9). These results show that the carbonyl stretch has a stronger absorbance than the O-H stretch, suggesting a slow reaction rate under these conditions. Similar results were observed for Trial 3 (50% THF) and Trial 4 (75% THF), (Figures 11 & 12 respectively), with stronger absorption by the carbonyl stretch compared to the O-H stretch. In contrast, the IR spectrum in Trial 2 show a greater absorption of O-H (78 %T) compared to the C=O stretch (86 %T) (Figure 10).

The results from Trial 2 indicate that this solvent ratio provided a good balance of solubility and proton transfer by IPA to the alkoxide intermediate.

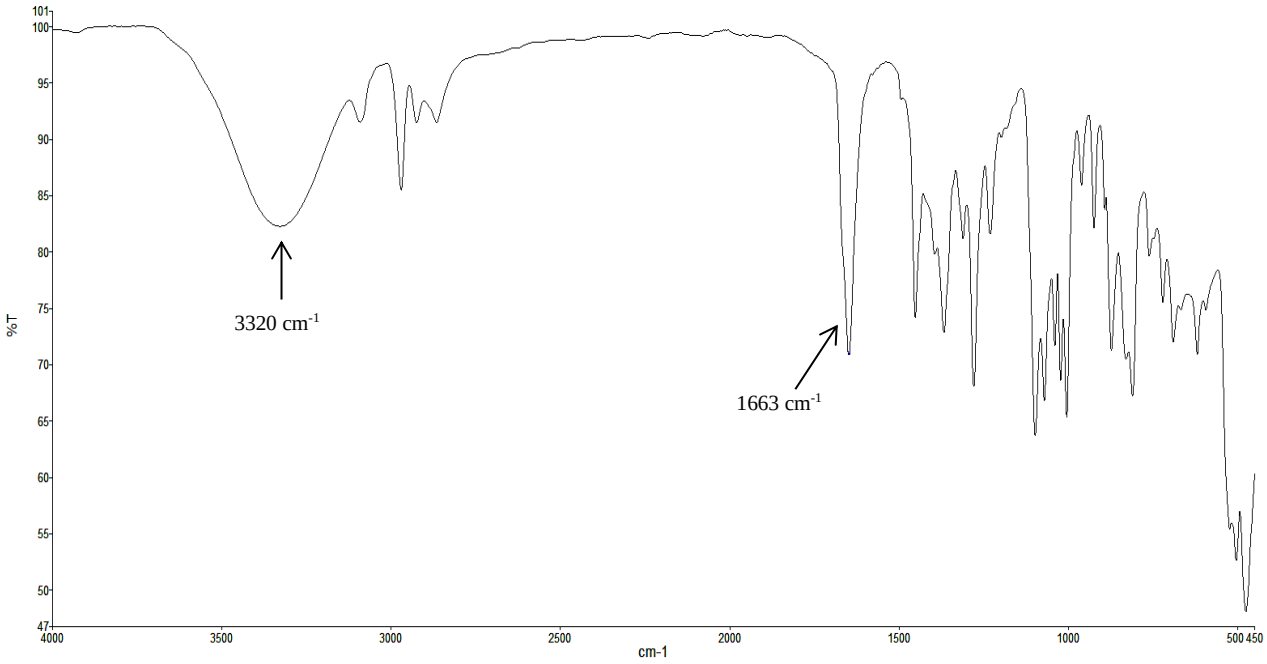

Figure 9: FT-IR Spectrum of Crude DHEFc, Trial 1: 0% THF

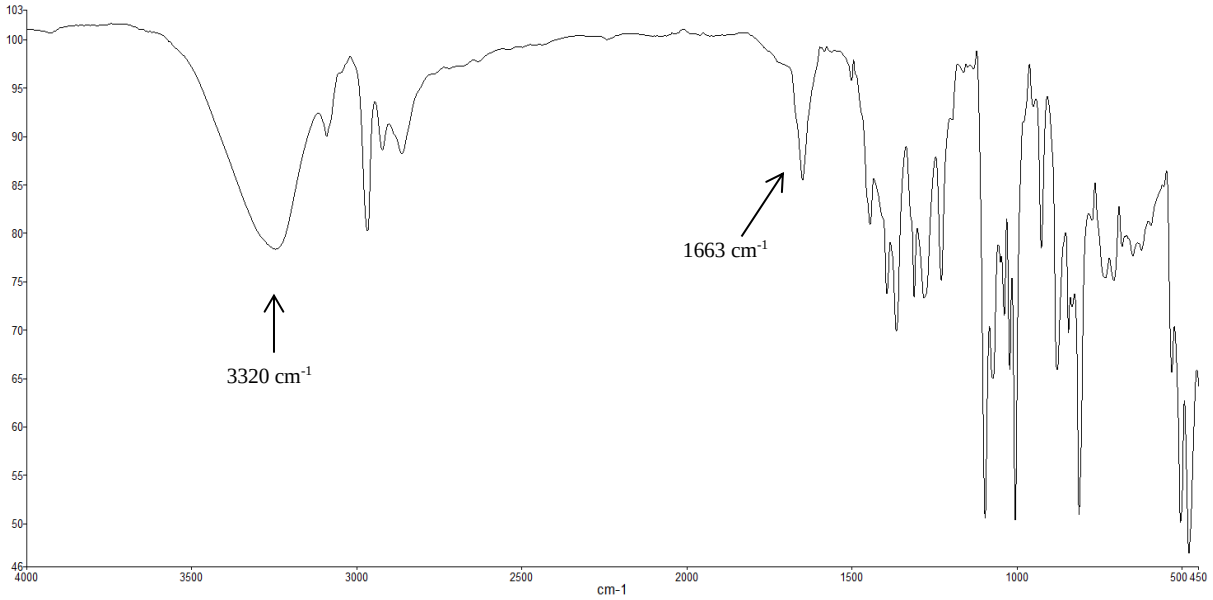

Figure 10: FT-IR Spectrum of crude DHEFc, Trial 2: 25% THF

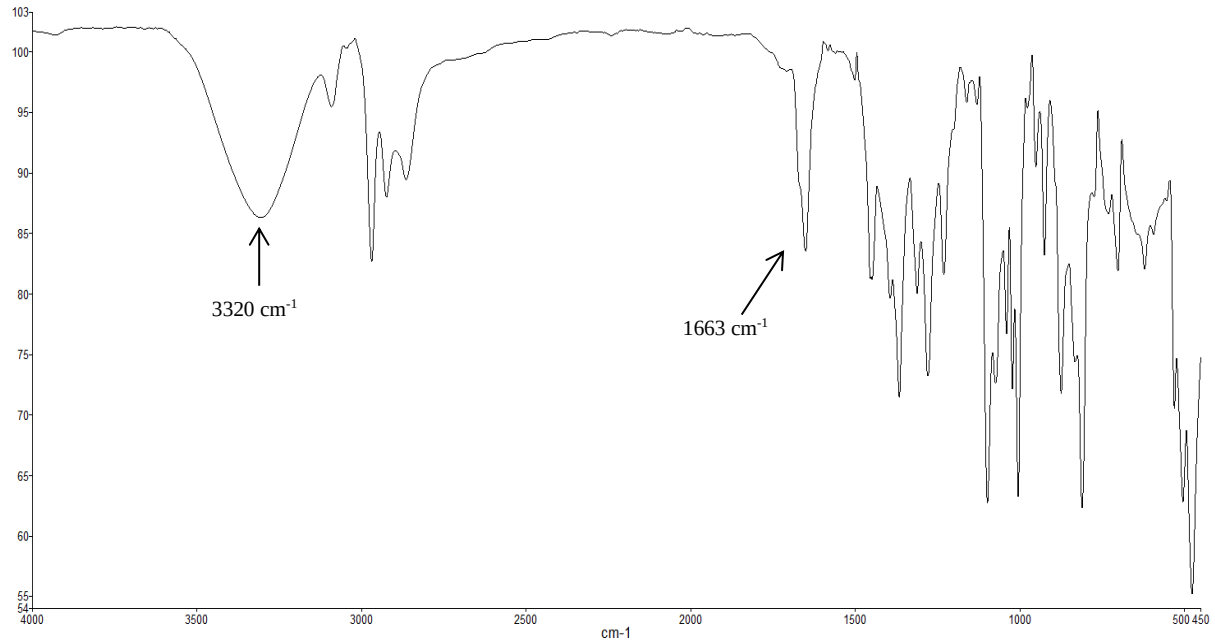

Figure 11: FT-IR Spectrum of crude DHEFc, Trial 3: 50% THF

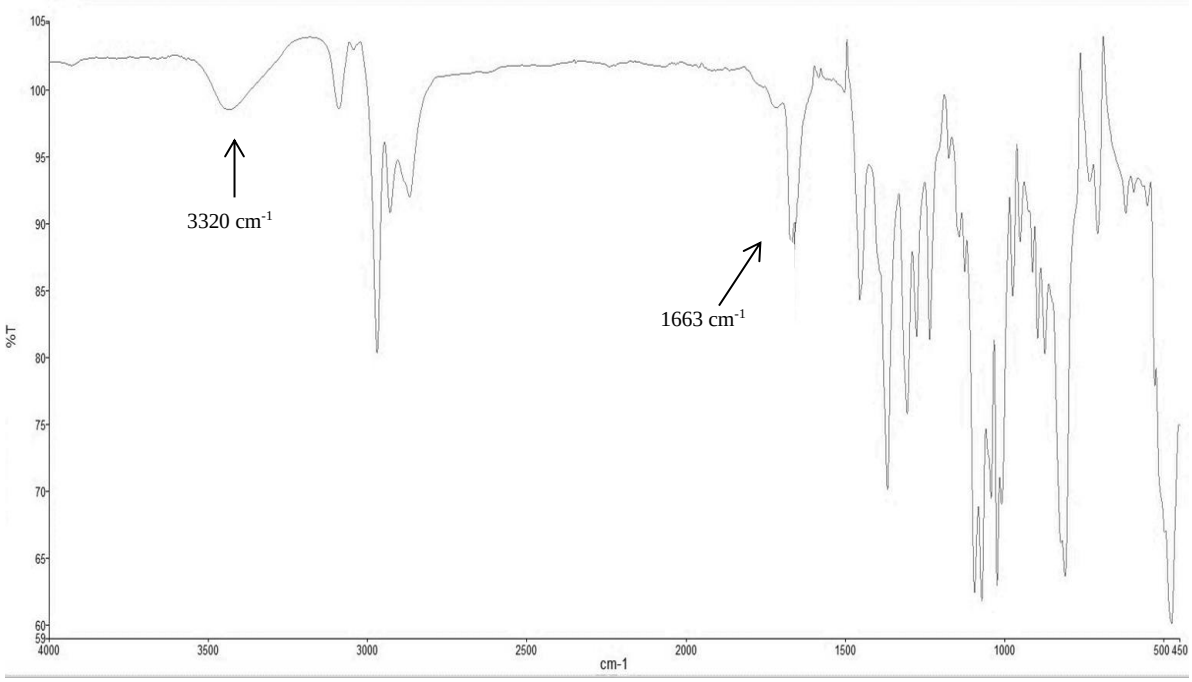

Figure 12: FT-IR Spectrum of crude DHEFc, Trial 4: 75% THF

3.1.4 Sodium Borohydride Parameters

Various amounts of $NaBH_4$ were used to determine the appropriate amount for effective reduction. Each trial used a THF:IPA ratio of 1:3 and reaction times of 16 hrs. Results were determined by following hydroxyl and carbonyl stretches in the IR spectrum (Table 2).

Table 2: Sodium Borohydride Optimization Parameters

Trial	1,1'-DAF:$NaBH_4$	O-H (%T*)	C=O(%T*)
1	1:2	83	70
2	1:3	78	0
3	1:4	78	0
4	1:5	78	0

* % transmittance

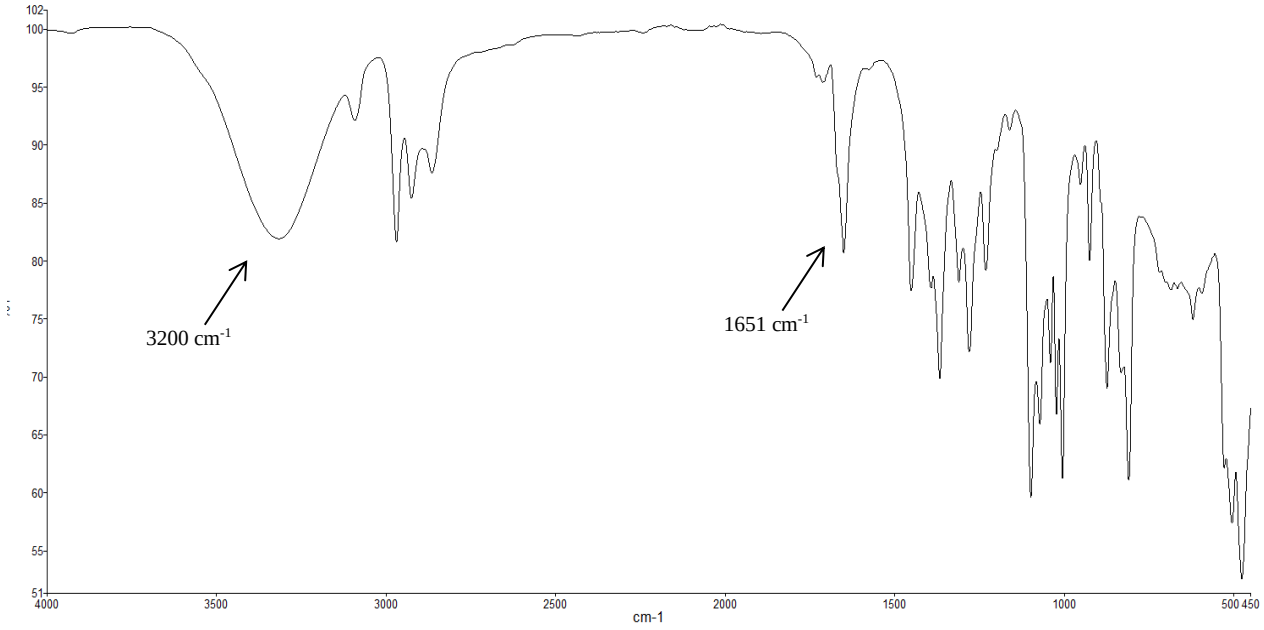

Figure 13: FT-IR Spectrum of DHEFc, Trial 1: 1:2 NaBH4

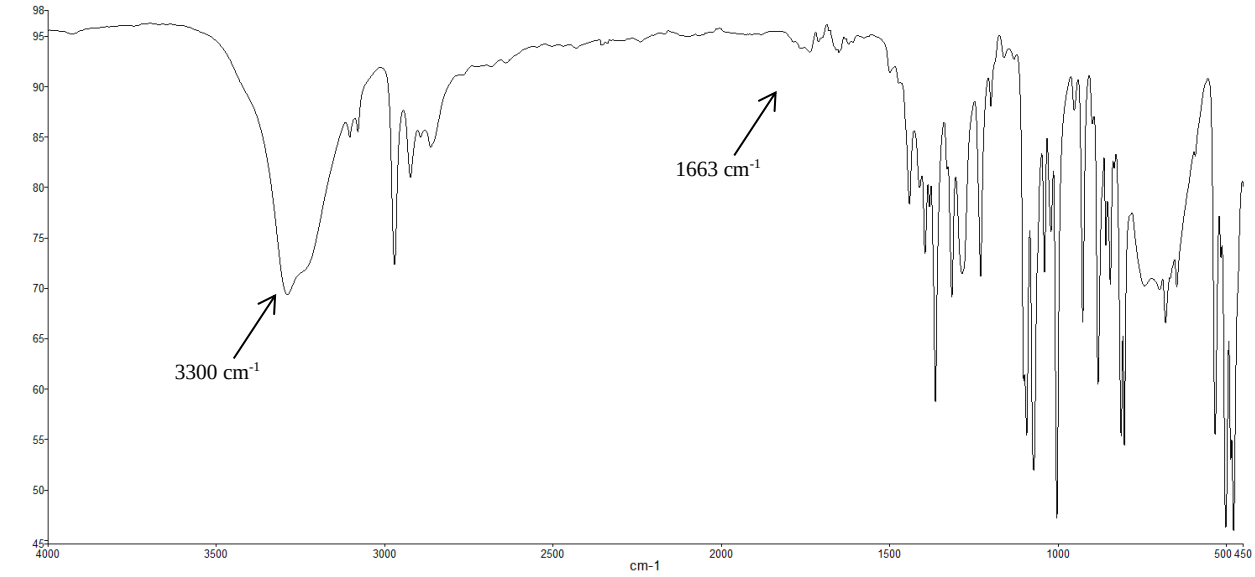

Figure 14: FT-IR Spectrum DHEFc, Trial 2:1:3 NaBH4

Trial 1 used a 1:2 molar ratio of 1,1'-DAF: $NaBH_4$ in solution (Table 2). A reduction of the ketone was observed at 1651.3 cm^{-1} (Figure 13) as well as a stretch attributed to the secondary alcohol was seen however the alcohol stretch was seen to be the weakest of all the trials indicating a slower reaction rate. Increasing the amount of sodium borohydride to a 1:3 ratio showed a full reduction was achieved in trial 2 (Figure 14). For trials 3 and 4, the results were consistent with trial 2 a complete reduction in the ketone. With these results a 1:3 ratio of DAF to $NaBH_4$ was determined to be sufficient.

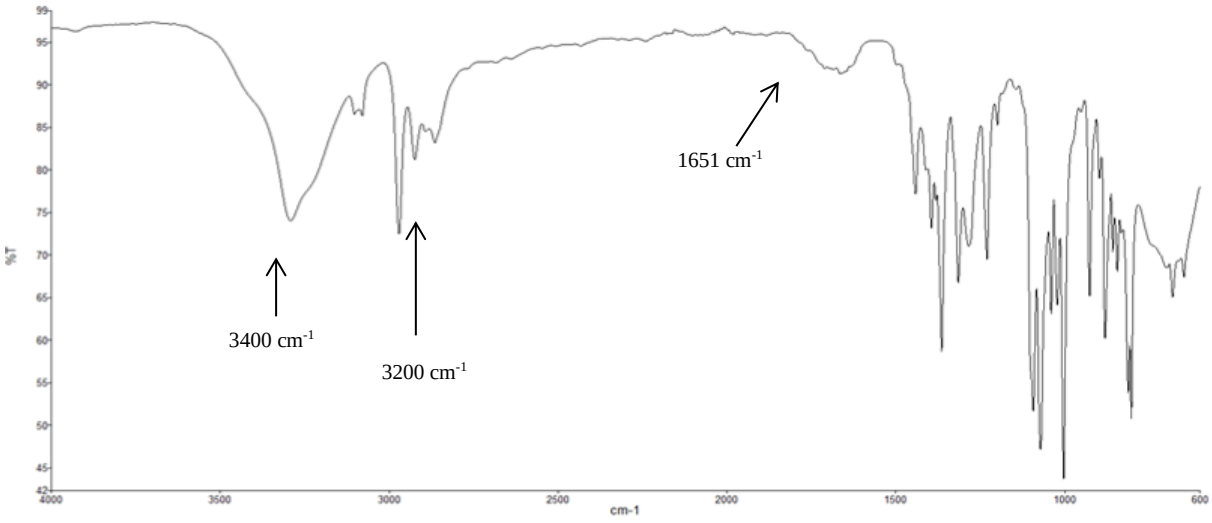

Figure 15: FT-IR Spectrum of DHEFc

3.2 DHEFc Characterization

To establish a successful reduction of 1,1'-DAF and the formation of a secondary alcohol, an FT-IR spectrum was analyzed (Figure 15). The reduction of the carbonyl peak at 1651 cm^{-1} was indicative of a successful reduction of the ketone group. The presence of a medium stretch occurring at 3400 cm^{-1} supports the formation of an alcohol functional group. Aromatic C-H bonding was seen at 3200 cm^{-1} confirming the presence

of ferrocene. Aliphatic C-H bonding was confirmed with peaks from ~2700 to 2900 cm^{-1} seen in the spectrum.

Proton NMR spectra were acquired to further validate a successful synthesis. An initial ^{1}H-NMR spectrum was acquired using $CDCl_3$ as the solvent (Figure 16). Two doublets seen at 1.466 ppm confirmed the presence of methyl protons. The presence of two peaks was thought to be attributed to the diastereomers that were formed since reduction of the carbonyls is not stereoselective. The cluster of signals seen at 4.101 ppm were ferrocenyl, methine, and hydroxyl protons (Figure 16).

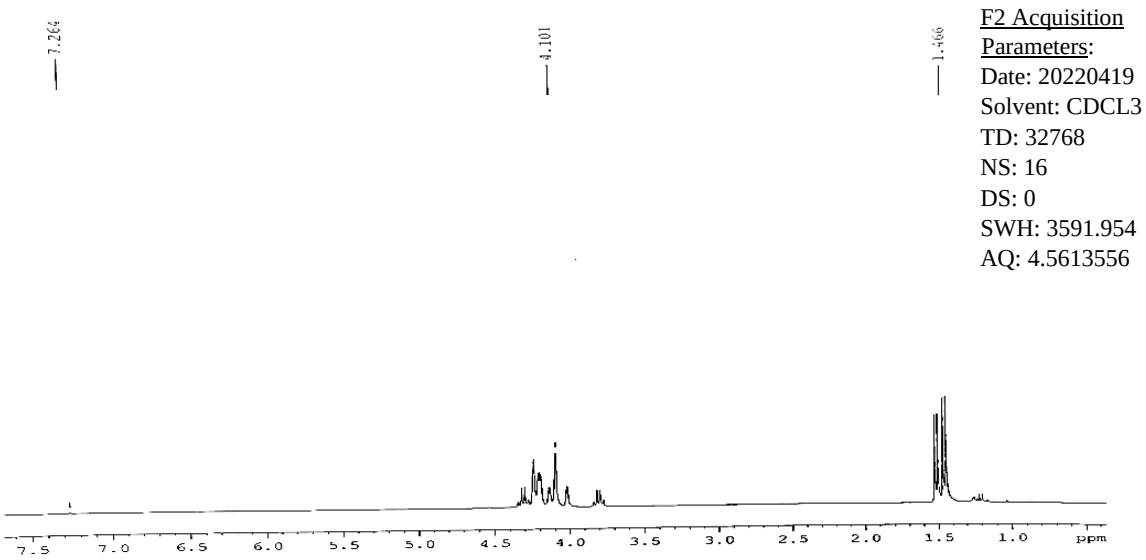

Figure 16: ^{1}H-NMR Spectrum of DHEFc ($CDCl_3$)

The spectrum of DHEFc in DMSO can be seen in Figure 17. It can be seen at 1.3 ppm the spectrum clarified the methyl proton splitting to be a doublet, being consistent with the structure of DHEFc. For the ferrocenyl protons appeared from 4.0-4.2 ppm

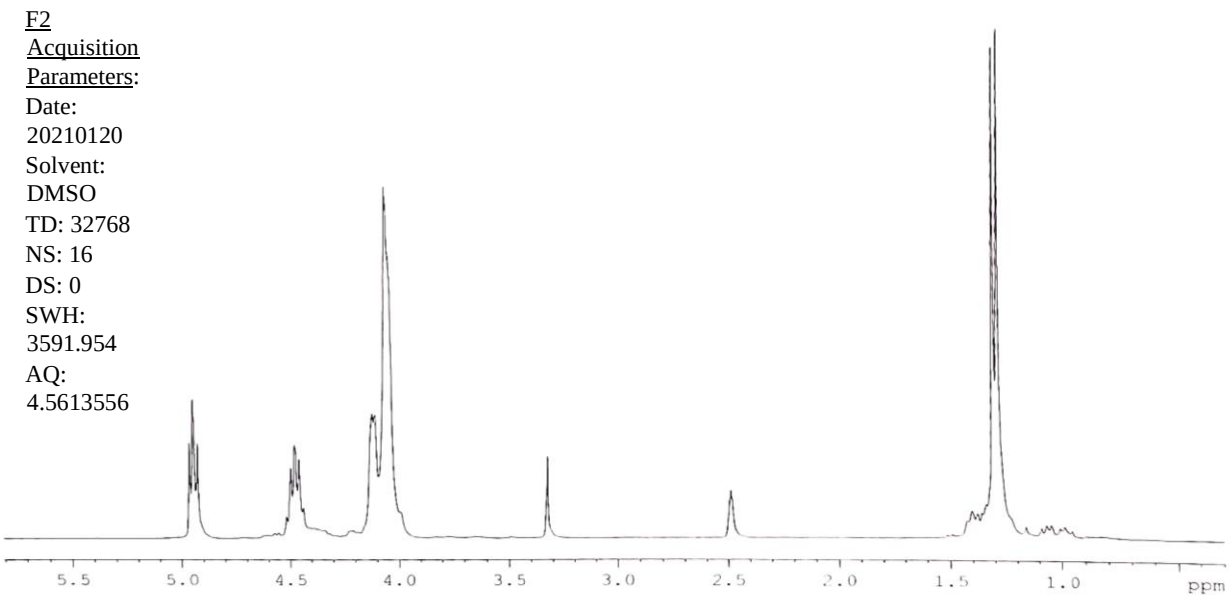

Figure 17: ^{1}H-NMR Spectrum of DHEFc (DMSO)

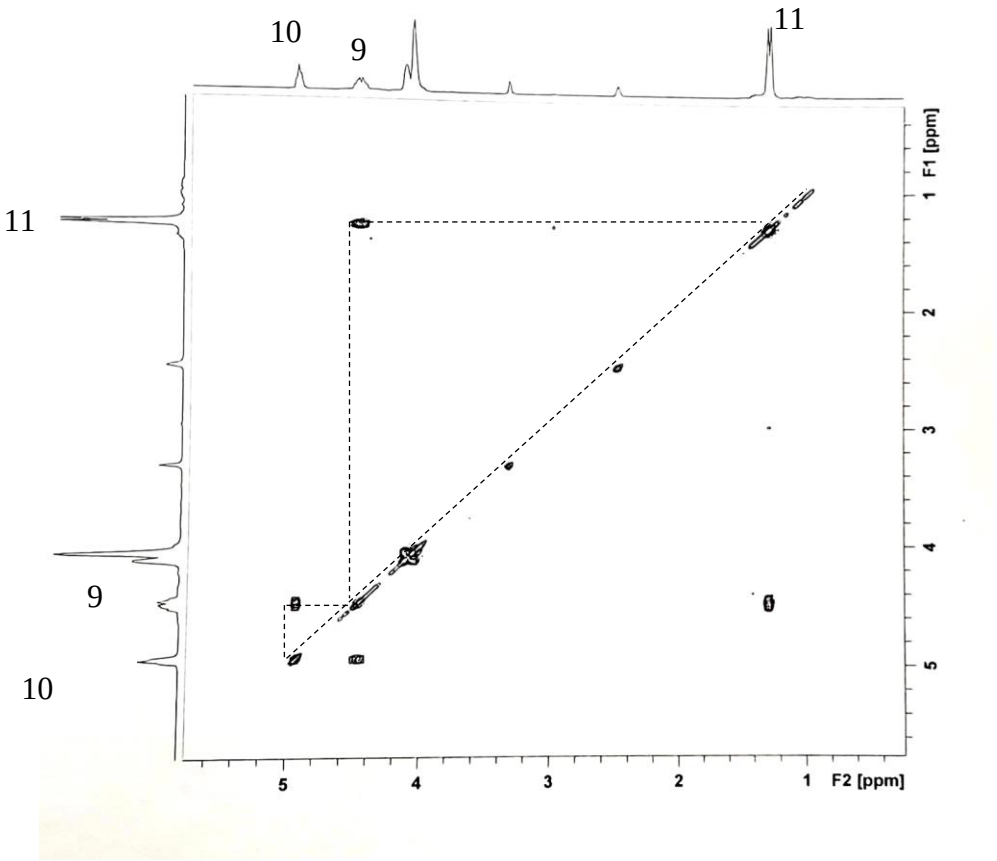

Figure 18: COSY Spectrum of DHEFc

A COSY spectrum was generated to assign the signals at 4.5 and 4.9 ppm (Figure 18). The signal at 4.5 ppm showed cross-peaks to the signals at 1.5 and 4.9 ppm indicating this signal is from the methine proton. The signal around 4.9 showed one cross-link peak as expected for the hydroxyl proton.

Lastly, the ^{13}C-NMR spectrum of DHEFc was obtained (Figure 19). The two methyl carbons are confirmed with signals occurring at 19.216 and 20.819 ppm. Methine carbons were observed at 63 and 65 ppm. Ferrocenyl carbons were confirmed with signals from 66 to 73 ppm. Signals at 88-90 ppm were attributed to substituted ferrocenyl carbons.

Due to the sensitivity of ^{13}C spectroscopy, the number of carbon signals seen was doubled due to the presence of diastereomers.

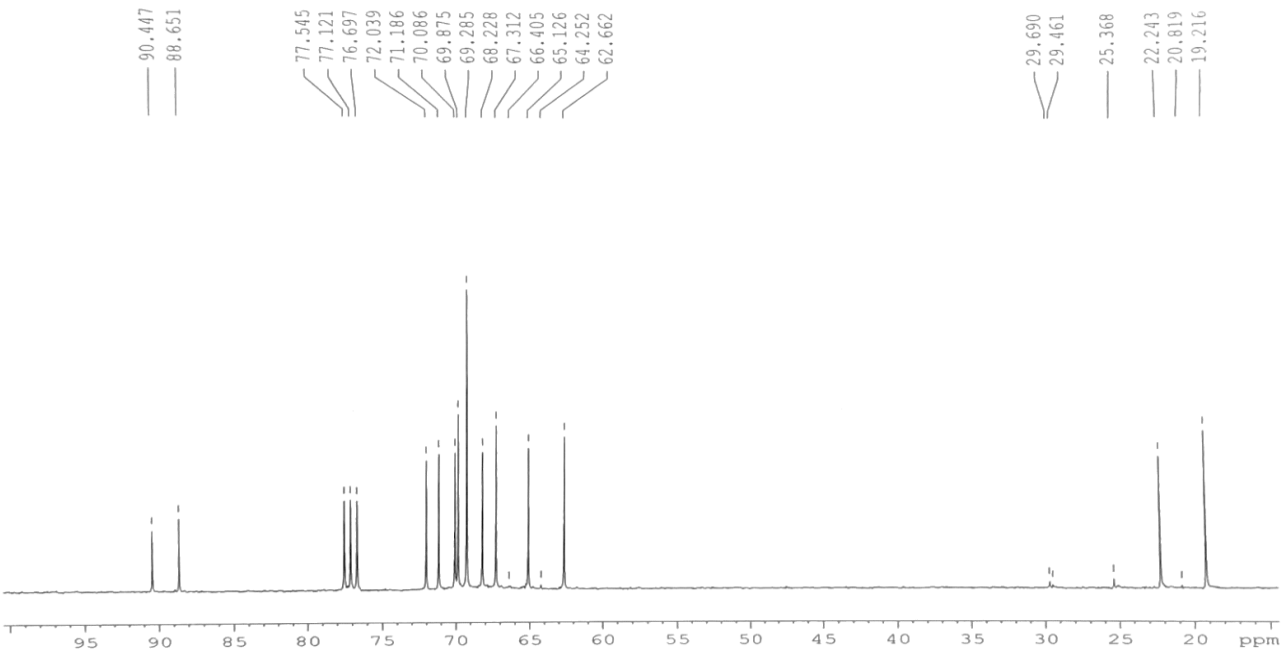

Figure 19: ^{13} C-NMR Spectrum of DHEFc

3.2.1 Polyurethane Films

Polyurethane films were formulated with various amounts of additive. The spectrum seen in Figure 20 represents the film cast with 20% DHEFc incorporated into the polyurethane film and similar spectra were obtained for the remaining films. An N-H stretch was observed at 3300 cm^{-1} along with an aliphatic C-H signal occurring at 2800 cm^{-1} and a C=O stretch at 1730 cm^{-1} were consistent with a polyurethane.

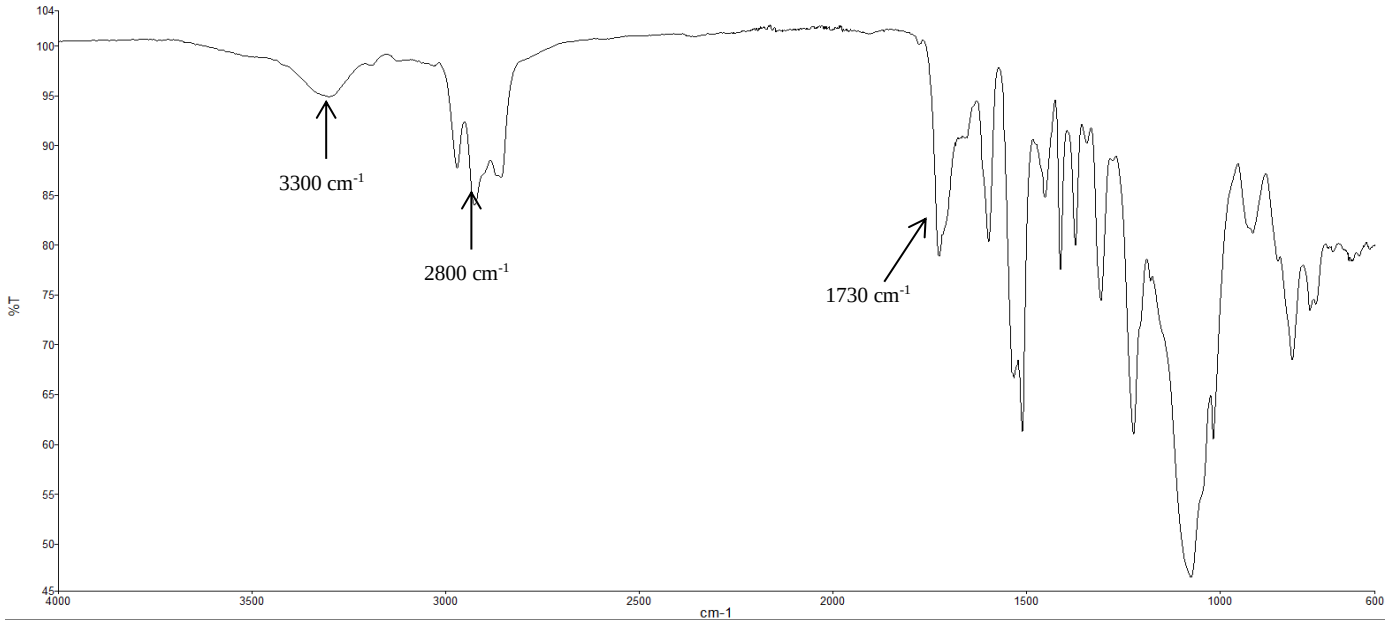

Figure 20: FT-IR Polyurethane Film

3.3 Horizontal Burn Testing

Thin films with varying amounts of additive were cast (Table 3) and burned in a vertical burn testing chamber. Final mass, burned mass and burn time will be reported.

Table 3: Polyurethane Thin Film Formulations

Trial	Polyol (g)	Isocyanate (g)	Additive (mole %)	Additive (g)
1	12.50	3.13	0	0
2	11.25	3.85	10	1.25
3	10.00	2.50	20	4.58
4	8.75	3.75	30	5.31

3.3.1 DHEFc Burn Test Results

Four trials were considered for testing (Table 4). A control PU film without DHEFc was considered and 100% of its mass was burned in 359.4 seconds. Trial 2 used a PU film with 10% DHEFc. An initial increase in time indicated the amount of DHEFc was not enough to reduce burn time effectively. However, the sample did exhibit a decrease in burned mass with 79.8% of the mass being burned. Trial 3 film used 20% of the additive DHEFc. A significant burn time reduction was observed, stopping the cycle of combustion in 131.5 seconds. It was also shown that 33.9% of the mass was burned continuing the trend of decreasing amounts of the sample being burned. Trial 4 used 30% DHEFc, continuing the trend of a significant decline in burn time, extinguishing the flame in 18.2 seconds as well as an acute decrease of 6.46% of the mass being burned.

Table 4: Horizontal Burn Test Results for Samples Containing DHEFc

Trial	DHEFc (g)	Initial Mass (g)	Final Mass (g)	Burned Mass (g)	Burned Mass (%)	Burn Time (sec)
1	0.00	2.43	-	2.43	100	359.4
2	1.25	2.23	0.451	1.78	79.8	371.4
3	2.50	2.01	1.33	0.681	33.9	131.5
4	3.75	2.54	2.38	0.164	6.46	18.2

3.3.2 HNT Burn Test Results

Burn testing of the HNT formulated thin films followed the same protocol as DHEFc thin films, results can be seen in Table 5. Trial one used 0% HNT determining a burn time of 350 seconds, burning 100% of the mass. When 10% HNT was used, the entire sample was consumed, however the burn time decreased to 280 seconds. Trial 3 used 20% HNT and an increase in burn time was observed, however 76.2% burned mass does indicate a decrease in burned mass from trial 2. Finally, 30% HNT was tested resulting in a further decrease in burned mass, 48.7%, but exhibiting a burn time of 524 seconds.

Table 5: Horizontal Burn Test Results for Samples Containing HNT

Trial	Halloysite (g)	Initial Mass (g)	Final Mass (g)	Burned Mass (g)	Burned Mass (%)	Burn Time (sec)
1	0.00	2.41	-	2.41	100	350
2	1.25	2.62	-	2.62	100	280
3	2.50	2.44	0.58	1.86	76.2	369
4	3.75	2.26	1.16	1.10	48.7	524

Burn mass vs. mass additive was plotted (Figure 21A) to investigate the amount of material burned once the combustion cycle had concluded. DHEFc exhibited an overall decrease in burned mass as the percentage of DHEFc increases with 6.46% of the mass being burnt at a 30% load (Table 3). HNT initially displayed an increase in burned mass indicating 10% HNT was not enough to exhibit desired FR properties. As the percentage of HNT increases, the plot decreases steadily with 30% HNT resulting in 48.7% of the sample being burned. DHEFc and HNTs showed efficacy in retaining mass as the percentage of the additive increases, however, DHEFc was shown to retain more mass within a shorter time frame than HNT.

Further analysis showed by plotting burn time vs. mass additive (Figure 21B). DHEFc exhibiting an increased in burn time initially followed by a significant decrease in burn time. The decrease in burn time continued throughout the sampling with 30% DHEFc demonstrating the most effective FR properties with a burn time of only 18.25 seconds. In comparison, HNT displays a slight decrease in burn time with a sharp increase as the percentage of HNTs was increased.

It is likely that DHEFc affects the vapor phase of combustion. These results indicate DHEFc shows efficacy in disrupting the radical process of combustion as the percentage of additive increases, with 30% DHEFc demonstrating the most promising results. When considering HNT, it is known that HNTs affect pyrolysis via char formation. Char formation is known to prevent fuel release as well as providing a thermal insulation layer for the sample. The experimental evidence indicated that HNT’s do not positively impact the burn time of a sample beyond a 10% load.

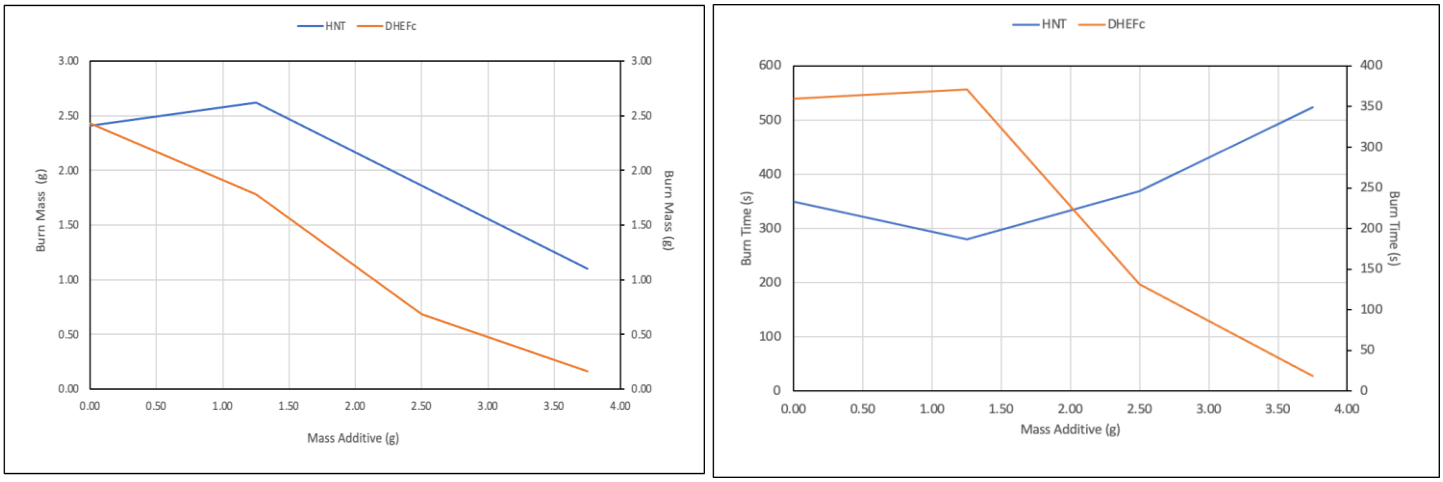

Figure 21: (A) Burned Mass vs Mass Additive; (B) Burn Time vs Mass Additive

3.3.3 DHEFc & HNT Burn Test Results

Burn testing of films containing DHEFc and HNT underwent the same procedure as previous experiments. Results can be seen in Table 6. Trial one used a 10:10 molar ratio of DHEFc and HNT within the PU film. It burn time of 11.3 seconds was observed with only 7.25% of mass burned. Trial two's film used a 10:30 molar ratio of DHEFc to HNT and resulted a dramatic increase in burn time as well as the burned mass percentage with 84.3% of the mass being lost over 357.2 seconds. Trial three increase the molar ratio to 20:20 with in 16.0% of burned mass in 53.68 seconds being observed. In trial four a burn time of 56.35 seconds was seen with 48.7% of the film mass lost. Trial five was observed to have 20.0% burned mass, decreasing from the previous trial however the burn time continued the increasing trend with a burn time of 64.08 seconds.

Table 6: DHEFc:HNT Horizontal Burn Test Results

Trial	Load Ratio	Mass Additive (g)	Initial Mass (g)	Final Mass (g)	Burned Mass (g)	Burned Mass (%)	Burn Time (sec)
1	10:10	2.50	2.00	1.8550	0.145	7.25	11.3
2	10:30	5.50	2.48	0.3901	2.090	84.3	357.2
3	20:20	5.00	4.29	3.52	0.770	18.0	53.68
4	30:10	5.00	4.80	4.15	0.650	13.5	56.35
5	30:30	7.50	2.90	2.32	0.58	20.0	68.40

Figures 23A and 23B compare the relationship between the mole percent ratios, burn time and percent burned mass. Initially, the trial one burned mass can be seen with only 0.145g of the film being burned with a burn time of 11.3 seconds being correlated. Trial two had a large increase in both burned mass as well as burn time with 2.090 g of the mass being burned in 357.2 seconds. A possible explanation for this observation is the char mechanism of the HNTs within the film dominated the FR properties of the ferrocene thus, elongating the burn time. Trial three and four had initial film masses of 5.00 however they were different formulations. Trial three had a 20:20 molar ratio burning 0.770 g of film mass being burnt in 53.68 seconds. Trial four, however, used a 30:10 molar ratio with 0.650 g of burned mass being observed in 56.35. The 2.67 second difference from each other indicates that a 20:20 molar ratio of DHEFc to HNT is comparable in burn time with a 30:10 molar ratio with the 30:10 ratio being preferred due to its ability to retain more of the mass. The 30:30 ratio showed an increase in burn time, however a decrease in burned mass is seen from trial 4. This would indicate that HNT can form an effective char layer retaining the mass however the FR properties of DHEFc seems to be dampened with the burn time increasing to 64.08 seconds.

These results would suggest that a low molar ratio of the two additives had constructive effects on the thin film preserving a majority of the sample with a burn time

of only 11.3 seconds. When DHEFc is the dominate additive, as seen in trial four, only 13.5% of the sample is burned giving the second-best burned mass results. Trial three and four have an interesting relationship regarding burn time. While trial three had the lower burn time (Table 3), it burned 18.0% of the sample mass. In comparison, trial four retained more mass with 13.5% of the sample being burned but an increased burn time is observed. Trial five showed a decrease in the burned mass and an increase in burn time indicative of DHEFc and HNT FR properties respectively, however the burned mass percentage increased to 20%.

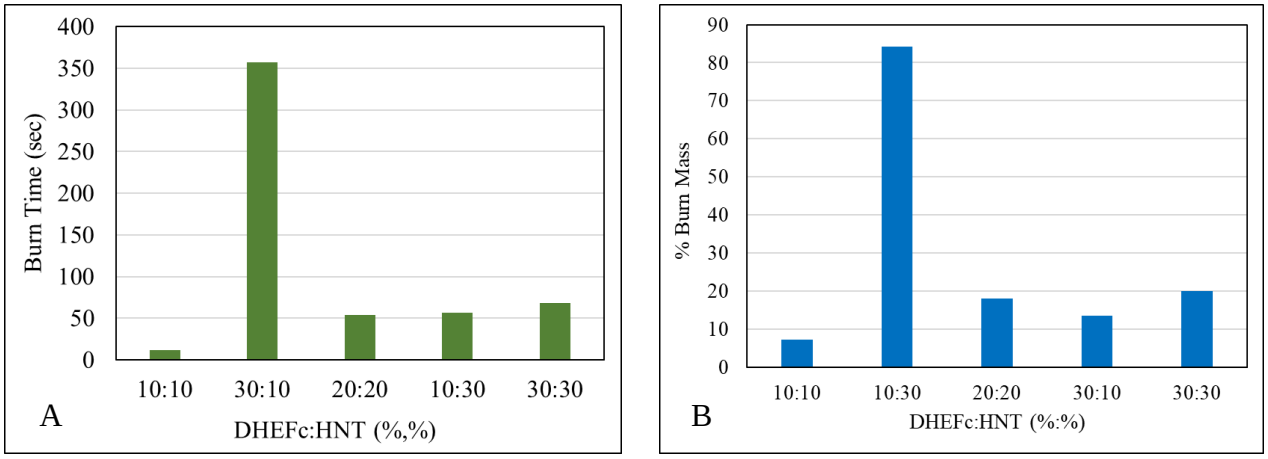

Figure 22: (A) Burn Time vs DHEFc:HNT Mole %, (B) DHEFc:HNT Burn Mass vs. Mole%

3.4 TGA Results

Thermal properties of samples containing 0, 10, 20 and 30 wt% additive were determined utilizing a ramp of 10 ^{o}C/ min up to 600 ^{o}C. Thermal stability at 10% weight loss, char yield and max derivative of weight were reported.

3.4.1 DHEFc TGA Results

The thermal stability (10% weight loss) of polyurethane films containing 0 - 30% DHEFc ranged from 203 - 282°C. Although the thermal stability did not show a consistent trend as DHEFc increased, the addition of DHEFc resulted in a loss of thermal stability. Interestingly, films containing DHEFc showed a slower decomposition (Figure 24A). With no DHEFc, the decomposition of the polyurethane begins ca. 250°C and ends ca. 350°C. However, the polyurethane with 10% DHEFc showed a decomposition that began at ca. 180°C and ended at ca. 400°C. While these results are not well understood, it may be due to ferrocene monomers being on the surface versus ferrocene monomers within the bulk of the film.

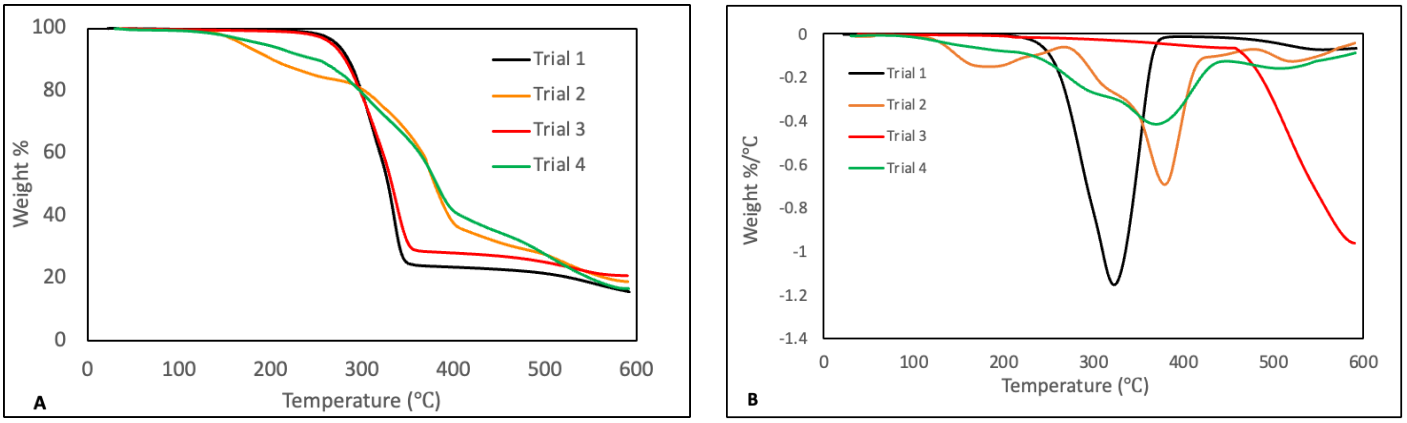

Figure 23: (A) DHEFc Degradation Curve, (B) DHEFc Derivative Plot

Presumably, decomposition of the DHEFc monomer occurs through heterolytic cleavage between the ferrocenyl carbon and the oxygen producing a relatively stable ferrocenyl carbocation. If these ferrocenyl compounds are on the surface then they would vaporize. However, within the bulk of the film, the ferrocenyl carbocation may be reacting with byproducts of the urethane thermal decomposition. It is well known that polyurethanes can thermally decompose into amines[48] and these amines may be

adding to the ferrocenyl carbocation, slowing the overall decomposition of the film. This was supported by the weight derivative curve. With no DHEFc, the fastest rate of decomposition occurred at ca. 320°C. In contrast, with the addition of DHEFc, the fastest rate of decomposition occurred at ca. 380°C, suggesting that stronger bonds are formed, slowing the decomposition process. Comparing char yields of this polymer series showed that char yield increased as the amount of DHEFc increased. These results are consistent with literature reports of ferrocene polymers showing good char yields[10]

Table 7: TGA Results of DHEFc

Trial	DHEFc (g)	Temperature at 10% wt. loss (°C)	Char Yield	Weight (% / °C)
1	0	285	15.6	325
2	1.25	202	18.8	382
3	2.50	281	20.8	469
4	3.75	250	16.6	376

3.4.2 Halloysite Nanotube TGA Results

The thermal stability (10% weight loss) of PU films containing 0-30% HNTs ranged from 282 – 285°C (Table 7). It is known that as a halogen free flame retardant HNTs can form a barrier between the polymer and the flame. In addition, halloysite is very thermally stable since it is an alumina silicate. Table 7 shows the results from the TGA of each sample. Addition of halloysite to the PU samples did not show a significant increase in thermal stability in the polymer. However, there was a substantial increase in char yield as the amount of halloysite increased. The increase in char yield was consistent since halloysite has been shown to be very thermally stable.

Table 8: TGA Results of HNT

Trial	HNT (g)	Temperature at 10% wt. loss (°C)	Char Yield (g)	Weight (%/°C)
1	0	285	15.6	326
2	1.25	282	20.3	382
3	2.50	283	26.0	329
4	3.75	285	26.2	332

3.4.3 DHEFc:HNT TGA Results

The thermal stability (10% weight loss) of the polyurethane films containing various molar ratios of DHEFc to HNT ranged from 219 – 281°C (Table 9). In samples 1 and 2 containing 10% DHEFc with 10% or 30% halloysite, respectively, the thermal stability was 272 and 282°C which indicates that the halloysite did not have a significant effect on the thermal stability. In contrast, higher loadings, 30%, of DHEFc with 10% or 30% halloysite showed lower thermal stabilities of 219 and 231°C in trials 4 and 5, respectively. This was consistent with films containing only DHEFc and may suggest that ferrocenyl moieties at the surface thermally decompose at lower temperatures.

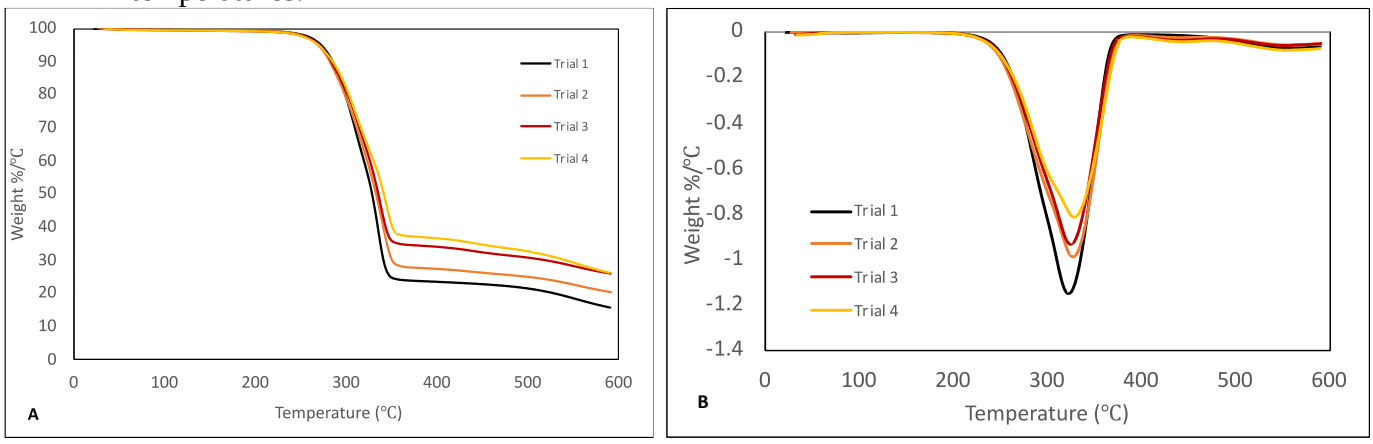

Figure 24: (A) HNT Degradation Curve, (B) HNT Derivative Plot

Comparing the Char Yields of Trials 1-5 showed that it generally increased as the amount of DHEFc or halloysite was increased. For the 10% DHEFc and 10% halloysite sample the char yielded was 18.6% and for the 30% DHEFc and 30% halloysite sample the char yielded was 29.1%. However, the halloysite seemed to have a larger effect on char yield with trial 2 (10% DHEFc and 30% halloysite) having a char yield of 26.8% and trial 4 (30% DHEFc and 10% halloysite) having a char yield of 22.6%.

In the weight derivative curves of each sample, two local maxima were observed. The first occurred at ca. 300^{o}C and the second occurred at ca. 384^{o}C. These results may be due to ferrocenyl moieties at the surface vs. in the bulk of the film, as was postulated for the DHEFc films. Ferrocenyl moieties at the surface will decompose first, while ferrocenyl groups in the bulk will react with byproducts of the polyurethane decomposition. Inclusion of halloysite may enhance this effect since it is well known to form a barrier layer which would explain two distinct maxima.

Table 9: TGA Results of DHEFc:HNT

Trial	DHEFc:HNT (%)	Temperature at 10% wt. loss (^{o}C)	Char Yield (g)	Weight (%/^{o}C)
1	10:10	272	18.6	382
2	10:30	282	26.8	381
3	20:20	282	27.7	384
4	30:10	219	22.7	384
5	30:30	231	29.1	387

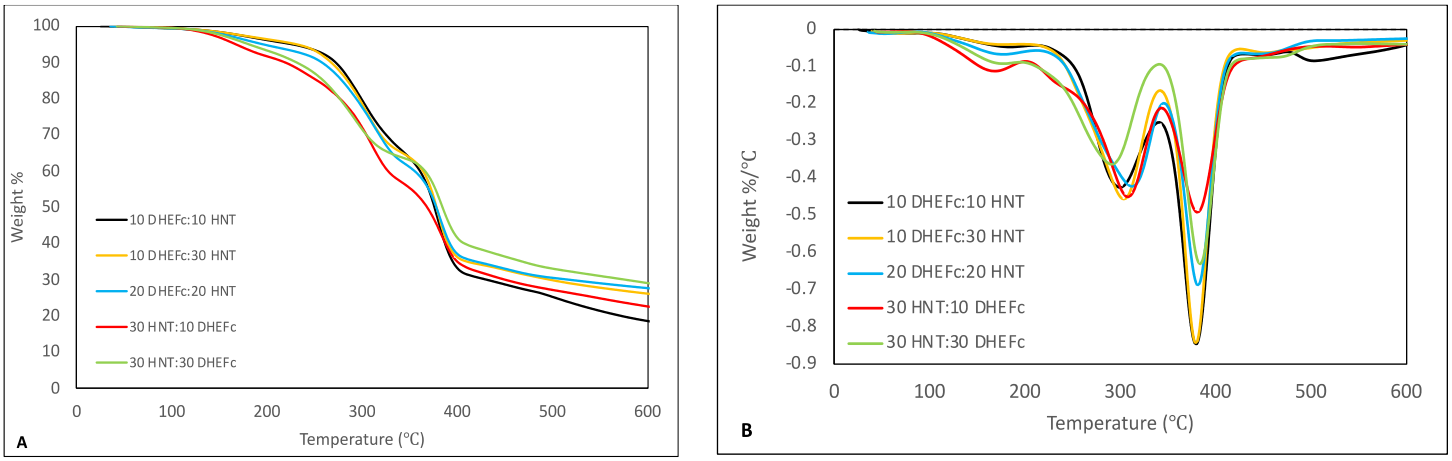

Figure 25: (A)DHEFc:HNT Degradation Curve, (B) DHEFc:HNT Derivative Plot

CHAPTER IV

CONCLUSION

When considering ferrocene as a flame retardant, DHEFc was shown to have efficacy. Optimized parameters were determined and resulted in a successful synthesis of DHEFc from 1,1-DAF. These results were confirmed via FT-IR, ^{1}H-NMR, ^{13}C-NMR, and COSY.

Thin film flame retardant properties were analyzed and determined DHEFc likely impacts the vapor phase of combustion with horizontal flame test burn times as low as 18.25 sec. Significant char formation determined via TGA confirmed ferrocene's known ability to impact this stage of combustion. Halloysite nanotubes demonstrated efficacy in forming a thermal insulation layer, however positive impact on the burn times was only seen up to a 10% loading.

Samples with both additives suggested that a 10:10 loading had the slowest burn times. Higher molar ratios longer burn times that were not fully understood. TGA analysis suggested surface ferrocenyl moieties decompose at lower thermal temperatures and that the addition of HNTs did not have a significant impact on the thermal stability. Char formation was determined to be positively impacted by an increase in additives. The observation of two local maxima in the derivative TGA curve, implied release of surface ferrocenyl moieties, demonstrated by the initial local

maxima followed by moieties within the bulk of the film yielding the second maxima. Results also suggested addition of HNTs enhanced this effect due to the known barrier formation capabilities.

Further research exploring discrepancies in burn testing and TGA data would be beneficial to further understand the flame retardancy mechanisms being demonstrated.

References

[1] Gama, N. V.; Ferreira, A.; Barros-Timmons, A. Polyurethane Foams: Past, Present, and Future. *Materials* **2018**, *11* (10), 1-2 https://doi.org/10.3390/MA11101841.

[2] McKenna, S. T.; Hull, T. R. The Fire Toxicity of Polyurethane Foams. *Fire Science Reviews 2016 5:1* **2016**, *5* (1), 1–27. https://doi.org/10.1186/S40038-016-0012-3

[3] Fortune Business Insight. *Polyurethane Market Size | Global Research Report [2021-2028]*. https://www.fortunebusinessinsights.com/industry-reports/polyurethane-pu-market-101801 (accessed 2022-04-04).

[4] *Flame Retardants for Fire Proof Plastics*. https://polymer-additives.specialchem.com/selection-guide/flame-retardants-for-fire-proof-plastics (accessed 2023-05-23).

[5] *Fire initiation and combustion process | Flame Retardants-Online*. https://www.flameretardants-online.com/fires/fire-initiation (accessed 2022-07-17).

[6] Giffin, M. *Ferrocene Incorporated Into Polyurethanes for Improved Flame-Retardant Properties*; 2016. https://digitalcommons.pittstate.edu/etd/91.

[7] Beard, A. Dr. *Intumescent flame retardant systems | Flame Retardants-Online*. Clariant Plastics & Coatings (Deutschland). https://flameretardants-online.com/flame-retardants/intumescence (accessed 2022-04-04).

[8] University of Pretoria. *Halogenated Flame Retardants*. Halogenated Flame Retardants. https://repository.up.ac.za/bitstream/handle/2263/22975/03chapter3.pdf?sequence=4&isAllowed=y (accessed 2023-05-23).

[9] Barnes, C. *What are Flame Retardant Polyurethanes?*. BBC Research. https://blog.bccresearch.com/what-are-flame-retardant-polyurethanes?msclkid=6be85c9fb09511ec96d37383c1d3453e (accessed 2022-04-05).

[10] Stoiber, T. Ph. D. *Study: Banned Since 2004, Toxic Flame Retardants Persist in U.S. Newborns | Environmental Working Group*. EWG. https://www.ewg.org/news-insights/news/study-banned-2004-toxic-flame-retardants-persist-us-newborns?msclkid=512ebd46b1f611ec87e28bd260ed1a3d (accessed 2022-04-04).

[11] Velencoso, M. M.; Battig, A.; Markwart, J. C.; Schartel, B.; Wurm, F. R. Molecular Firefighting—How Modern Phosphorus Chemistry Can Help Solve the Challenge of Flame Retardancy. *Angewandte Chemie International Edition* **2018**, *57* (33), 10450– 10467. https://doi.org/10.1002/ANIE.201711735.

[12] Kirman, J. *Polyfluoroalkylphosphorus Compounds - ProQuest*. https://www.proquest.com/docview/2619239186?pq-origsite=gscholar&fromopenview=true (accessed 2023-05-10).

[13] Beach, M. W.; Kearns, K. L.; Davis, J. W.; Stutzman, J. R.; Lee, D.; Lai, Y.; Monaenkova, D.; Kram, S.; Hu, J.; Lukas, C. Stability Assessment of a Polymeric Brominated Flame Retardant in Polystyrene Foams under Application-Relevant Conditions. *Environ Sci Technol* **2021**, *55* (5), 3050–3058. https://doi.org/10.1021/acs.est.0c04325.

[14] Markwart, J. C.; Battig, A.; Zimmermann, L.; Wagner, M.; Fischer, J.; Schartel, B.; Wurm, F. R. Systematically Controlled Decomposition Mechanism in Phosphorus Flame Retardants by Precise Molecular Architecture: P–O vs P–N. *ACS Appl. Polym. Mater.* **2019**, *1* (5), 1118–1128. https://doi.org/10.1021/acsapm.9b00129.

[15] Morgan, A. B. A Review of Transition Metal-Based Flame Retardants: Transition Metal Oxide/Salts, and Complexes. In *ACS Symposium Series*; American Chemical Society, 2009; Vol. 1013, pp 312–328. https://doi.org/10.1021/bk-2009-1013.ch019.

[14] Werner, H. At Least 60 Years of Ferrocene: The Discovery and Rediscovery of the Sandwich Complexes. *Angewandte Chemie International Edition* **2012**, *51* (25), 6052–6058. https://doi.org/10.1002/ANIE.201201598.

[15] Linteris, G. T.; Rumminger, M. D.; Babushok, V.; Tsang, W. Flame Inhibition by Ferrocene and Blends of Inert and Catalytic Agents; 2000; Vol. 28, pp 2965–2972.

[16] Vahabi, H.; Sonnier, R.; Taguet, A.; Otazaghine, B.; Saeb, M. R.; Beyer, G. Halloysite Nanotubes (HNTs)/Polymer Nanocomposites: Thermal Degradation and Flame Retardancy. *Clay Nanoparticles* **2020**, 67–93. https://doi.org/10.1016/B978-0-12- 816783-0.00003-7.

[17] Hong, N.; Song, L.; Hull, T. R.; Stec, A. A.; Wang, B.; Pan, Y.; Hu, Y. Facile Preparation of Graphene Supported Co3O4 and NiO for Reducing Fire Hazards of Polyamide 6 Composites. *Materials Chemistry and Physics* **2013**, *142* (2–3), 531–538. https://doi.org/10.1016/J.MATCHEMPHYS.2013.07.048.

[18] Werner, H. At Least 60 Years of Ferrocene: The Discovery and Rediscovery of the Sandwich Complexes. *Angewandte Chemie International Edition* **2012**, *51* (25), 6052–6058. https://doi.org/10.1002/ANIE.201201598.

[19] Linteris, G. and Rumminger, M. (1999), Flame Inhibition by Ferrocene, Carbon Dioxide, and Trifluoromethane Blends: Synergistic and Antagonistic Effects, Chemical and Physical Processes in Combustion. *Combustion Institute/Eastern States Section*,

Raleigh, NC, [online], https://tsapps.nist.gov/publication/get_pdf.cfm?pub_id=914176 (Accessed July 26, 2023)

[20] Linteris, G. T.; Rumminger, M. D.; Babushok, V.; Tsang, W. Flame Inhibition by Ferrocene and Blends of Inert and Catalytic Agents. *Proceedings of the Combustion Institute* **2000**, *28* (2), 2965–2972. https://doi.org/10.1016/S0082-0784(00)80722-5.

[21] Du, M.; Guo, B.; Jia, D. Newly Emerging Applications of Halloysite Nanotubes: A Review *Polymer International* **2010**, *59* (5), 574–582. https://doi.org/10.1002/PI.2754.

[22] Vahabi, H.; Sonnier, R.; Taguet, A.; Otazaghine, B.; Saeb, M. R.; Beyer, G. 3 - Halloysite Nanotubes (HNTs)/Polymer Nanocomposites: Thermal Degradation and Flame Retardancy. In *Clay Nanoparticles*; Cavallaro, G., Fakhrullin, R., Pasbakhsh, P., Eds.; Micro and Nano Technologies; Elsevier, 2020; pp 67–93. https://doi.org/10.1016/B978-0-12-816783-0.00003-7.

[23] Ma, W.; Wu, H.; Higaki, Y.; Takahara, A. Halloysite Nanotubes: Green Nanomaterial for Functional Organic-Inorganic Nanohybrids. *The Chemical Record* **2018**, *18* (7–8), 986–999. https://doi.org/10.1002/tcr.201700093.

[24] Technology, M. I. of. Experiment #4: The Preparation of Ferrocene & Acetylferrocene The Preparation of Ferrocene Acetylferrocenes 1. **1952**, 1–20

[25] Intertek. *ASTM D635: Rate of Burning and/or Extent and Time of Burning of Plastics in a Horizontal Position*. https://www.intertek.com/building/standards/astm-d635/ (accessed 2022-04-02).

[26] SDL Atlas Textile Testing Solutions. *Vertical Flammability Chamber | Textile Testing Products | SDL Atlas*. https://sdlatlas.com/products/vertical-flammability-chamber#product-details (accessed 2022-04-02).